



Original article

Synthesis, physicochemical properties of allopurinol derivatives and their biological activity against *Trypanosoma cruzi*M.A. Raviolo ^{a,*}, M.E. Solana ^{b,2}, M.M. Novoa ^{b,2}, M.S. Gualdesi ^{a,1}, C.D. Alba-Soto ^{b,2}, M.C. Briñón ^{a,*}^a Departamento de Farmacia, Facultad de Ciencias Químicas, Universidad Nacional de Córdoba, 5000 Córdoba, Argentina^b Instituto de Microbiología y Parasitología Médica (IMPaM-UBA-CONICET), Facultad de Medicina, Universidad de Buenos Aires, 1121 Ciudad Autónoma de Buenos Aires, Argentina

ARTICLE INFO

Article history:

Received 30 May 2013

Received in revised form

28 August 2013

Accepted 31 August 2013

Available online 13 September 2013

Keywords:

Trypanosoma cruzi

Allopurinol derivatives

Physicochemical properties

Trypanocidal activity

ABSTRACT

Chagas disease is caused by *Trypanosoma cruzi* (*T. cruzi*) leading to a huge number of infections and deaths per year, because in addition to many sufferers only having limited access to health services only an inefficient chemotherapy is available using drugs such as benznidazole and nifurtimox. Here, C6-alkyl (**2a–c**) and N1-acyl (**3a–c**) derivatives of Allopurinol (Allop, compound with activity against *T. cruzi*) were synthesized in good yields and their structures were unambiguously characterized. Only **2a**, **2b** and **3c** showed inhibitory activity against the proliferative stages of the parasite when tested at $1 \mu\text{g mL}^{-1}$ with the **3c** derivative exhibiting an IC₅₀ value similar to that of Allop and not being toxic for mammalian cells. Relevant pharmaceutical physicochemical properties (pKa, stability, solubility, lipophilicity) were also determined as well by using Lipinski's rule, polar surface area and molecular rigidity. Taken together, the results demonstrated that the studied derivatives had optimal properties for bioavailability and oral absorption. For the stability studies, Micellar Liquid Chromatography was used as the analytical method which was fully validated according to the FDA guidelines and shown to be a suitable, sensitive and simple method for routine analysis of these Allop derivatives.

© 2013 Elsevier Masson SAS. All rights reserved.

1. Introduction

Chagas disease (Chagas) or American Trypanosomiasis is caused by the protozoan *Trypanosoma cruzi* (*T. cruzi*), and remains a major health problem in Central and South America that affects nearly 8–10 million people throughout Latin America [1].

In endemic countries, *T. cruzi* is transmitted via haematophagous triatomine insect vectors that release infective forms within the feces and urine after every mammalian blood ingestion. Once in the host, parasites invade cells and undergo differentiations into intracellular amastigotes (AMAS), which after several rounds of duplication transforms them into trypomastigotes (TRYP), the form that disseminates the infection. Transmission may also occur through laboratory accidents, organ transplantation,

ingestion of contaminated food as well as by blood transfusion and congenital passage [1]. The global increase in human migrations is responsible for most of the cases reported in non-endemic countries [2].

Paradoxically, 100 years after the first report describing the morphology and the life cycle of the pathogen, neither vaccines nor effective treatments for chronic cases are available. One reason for this may be that Chagas disease belongs to a group of tropical infections that are endemic mainly among low-income populations of the developing regions of Africa, Asia, and America, which are named *neglected diseases* [3]. The lack of interest of pharmaceutical companies and the absence of effective social policies from the affected states are responsible for the limited evolution toward an improved pharmacotherapy.

Chagas disease initiates as an acute phase that is usually asymptomatic. Then, after decades of chronic infection, 30–40% of the infected people develop symptoms that can include cardiac and/or digestive (megaesophagus or megacolon) forms. Despite significant progress having been made in understanding the biochemistry and physiology of the causative agent, the current etiological treatment of Chagas disease is based on rather

* Corresponding authors. Tel.: +54 351 5353865; fax: +54 3515353364.

E-mail addresses: moraviolo@fcq.unc.edu.ar (M.A. Raviolo), macribr@fcq.unc.edu.ar (M.C. Briñón).¹ Tel.: +54 351 5353865x53355.² Tel.: +54 11 59509500x2189; fax: +54 11 59509577.

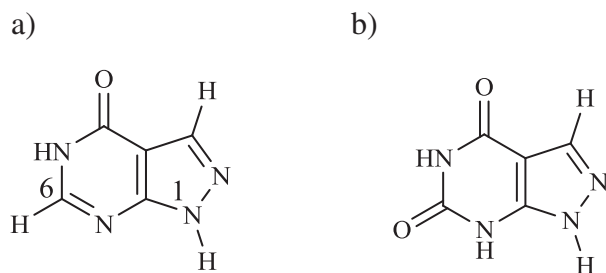


Fig. 1. Allopurinol (a) and its metabolite oxypurinol (b).

unspecific drugs developed more than four decades ago, such as nifurtimox and benznidazole (Bz). Moreover, although the use of these drugs to treat the acute phase of the disease is widely accepted, etiological treatment at the chronic phase remains controversial [4], with the undesirable side effects of both drugs being major drawbacks and frequently forcing treatment to be discontinued [5]. Research on anti-*T. cruzi* compounds has been to date based on different strategies aimed at targeting specific parasite enzymes or parasite DNA or at inducing oxidative stress damage [6,7].

Nevertheless, the development of safer and more efficient trypanocidal drugs remains a major goal in Chagas disease chemotherapy, with one possibility being to exploit differences in the purine metabolism between *T. cruzi* and host cells. Although *T. cruzi* does not synthesize purines *de novo* as in the case of mammals, the parasite is able to concentrate the pyrazolopyrimidines within the cell and metabolize them as purines through a salvage pathway, ultimately incorporating them into nucleic acids [8,9].

Allopurinol (**1**, Allop 1,5-dihydro-4*H*-pyrazolo[3,4-*d*]pyrimidin-4-one, Fig. 1a) employed for the treatment of hyperuricemia, is an hypoxanthine analog used by the *T. cruzi*'s hypoxanthine–guanine phosphoribosyltransferase (HGPRT) as an alternative substrate. This enzyme can incorporate Allop into the parasite's ribonucleic acid as a non-physiological nucleotide; thus blocking the synthesis of new purine nucleotides [10,11]. The activity of Allop in chemotherapy for Chagas disease has been extensively investigated, but the results are somewhat contradictory [12–14]. In a recent pilot study, Perez-Mazliah et al. [15] showed that the combination of Allop and Bz induced significant modifications of the T and B cell

responses, indicative of a reduction of the parasite burden, and thereby sustained the feasibility of administration of two antiparasitic drugs in the chronic phase of Chagas disease. In addition, these two drugs when administered together were reported to be safe and effective in the treatment of Chagas disease reactivation after heart transplantation [16].

The variable efficacy of Allop depends on the infective parasite population, which varies among geographical areas [17]. In addition, in mammals, Allop is converted into oxypurinol by xanthine oxidase (Fig. 1b) with a $t_{1/2} = 1\text{--}2$ h, which is not a substrate for HGPRT and has no anti-*T. cruzi* activity [10].

Although Allop presents trypanocidal activity, its failure in avoiding Chagas disease progression may be due in part to inadequate blood levels caused by unfavorable physicochemical properties, thus leading to versatile responses in humans.

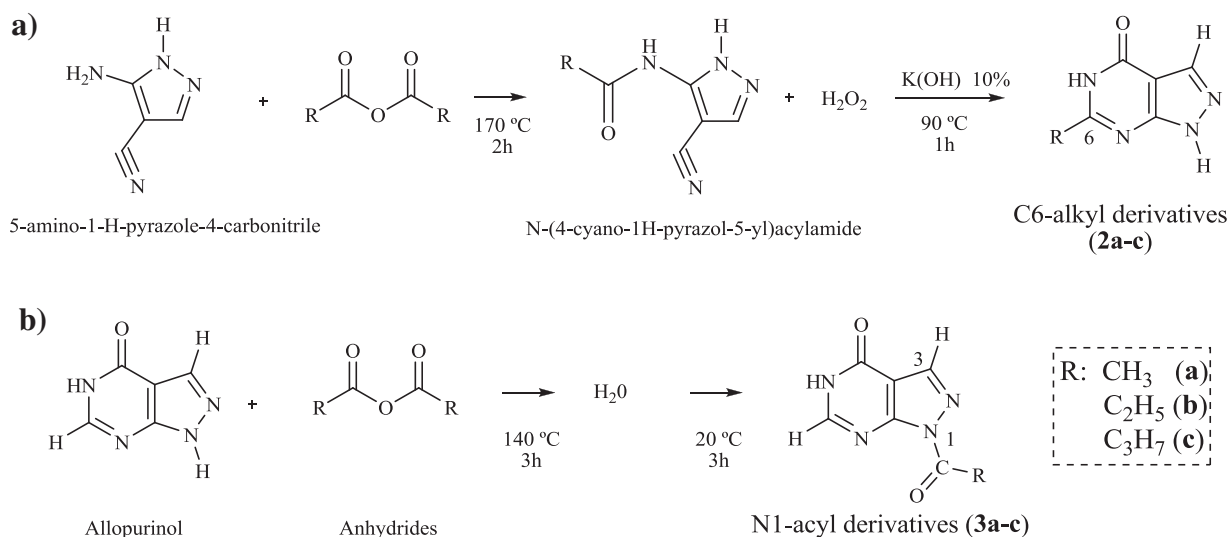
In an attempt to improve its performance, we have developed a series of derivatives of Allop by chemical modification of their specific functional groups, resulting in active anti-*T. cruzi* agents *per se* or prodrug compounds. Then, their activities against *T. cruzi* as well as their different relevant physicochemical properties, such as their integrity in buffers, simulated fluids and human plasma were determined, in addition to carrying out hydrolytic and oxidative studies, and determining acid dissociation constants, lipophilicity and solubility.

2. Results and discussion

2.1. Chemistry

Taking into account that C6 of Allop is a target of metabolism for the xanthine oxidase enzyme, a series of derivatives with alkyl groups on this position (**2a–c**) were synthesized in two steps, obtaining 6-methyl-1,5-dihydro-4*H*-pyrazolo[3,4-*d*]pyrimidin-4-one (**2a**), 6-ethyl-1,5-dihydro-4*H*-pyrazolo[3,4-*d*]pyrimidin-4-one (**2b**) and 6-propyl-1,5-dihydro-4*H*-pyrazolo[3,4-*d*]pyrimidin-4-one (**2c**) by employing the method of Cheng and Robins [18] (Scheme 1a). It is important to point out that Biagi et al. have found that these compounds to be ineffective inhibitors of this enzyme, and that neither physicochemical properties nor activity against *T. cruzi* were previously studied [19].

N1-acyl prodrugs of Allop were also synthesized (**3a–c**) to improve their physicochemical properties; whose design was based



Scheme 1. Synthesis procedures used for the development of derivatives. a) C6-alkyl derivatives of Allop (**2a–c**), b) N1-acyl derivatives of Allop (**3a–c**).

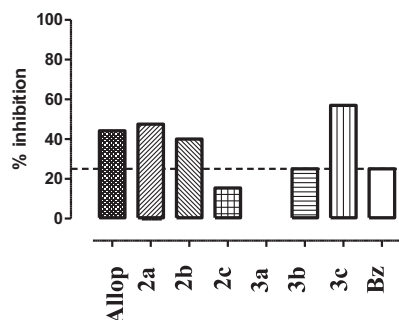


Fig. 2. Growth inhibition of *T. cruzi* amastigotes by C6-Alkyl (**2a–c**) and N1-Acyl (**3a–c**) derivatives of Allopurinol. AMAS were cultured in Vero cell monolayers in the presence of $1 \mu\text{g mL}^{-1}$ of each compound. The graph represents the rate of growth inhibition related to untreated *T. cruzi*-infected cells (0%). Data are representative of two independent experiments. The dashed line shows the effect of Benznidazole (Bz) as the reference drug. Derivatives were selected on the basis of their behavior compared to Bz.

on the removal of the NH-acidic proton. Thus, N1-acyl derivatives of Allop, 1-acetyl-1,5-dihydro-4*H*-pyrazolo[3,4-*d*]pyrimidin-4-one (**3a**), 1-propanoyl-1,5-dihydro-4*H*-pyrazolo[3,4-*d*]pyrimidin-4-one (**3b**) and 1-butanoyl-1,5-dihydro-4*H*-pyrazolo[3,4-*d*]pyrimidin-4-one (**3c**) were prepared according to the Bundgaard procedures (Scheme 1b) [20]. In this way, one hydrogen bond donor group was eliminated, thereby having a significant effect on relevant properties such as crystal lattice energy, solubility, dissolution rate, and permeability [21].

The structures of compounds **2a–c** and **3a–c** were characterized by high resolution mass spectrometry and spectroscopic methods. ^1H NMR, ^{13}C NMR, HSQC-DEPT (Heteronuclear Single Quantum Correlation-Distortionless Enhancement by Polarization Transfer) and HMBC (Heteronuclear Multiple Bond Correlation) of **2a–c** and **3a–c** were performed on DMSO- d_6 . Although these compounds have been previously reported, the NMR bidimensional techniques allowed us to unequivocally reassign the chemical shifts of **3a–c** to those reported by Bundgaard and Falch [20]. In this way, in the only two protons of Allop bonded to carbon atoms (CH) (H-6, δ 8.40 and H-3, δ 8.34), an inversion of their chemical shifts was observed in **3a–c** derivatives, leading to signals for H-3 and H-6 of δ 8.35 \pm 0.01 and δ 8.28, respectively. In addition, the structure of **2a–c** was confirmed by the HSQC-DEPT technique, thereby showing that C-6 is a quaternary carbon. All the ^1H and ^{13}C NMR data of the compounds given in the Experimental section are in full agreement with the proposed structures, with the representative HSQC-DEPT and HMBC for Allop, **2c** and **3c** being shown in the Supplementary Materials.

2.2. Activity

The inhibitory effect of each C6-alkyl- and N1-acyl derivative of Allop against TRYP was measured, but no compound displayed any consistent trypanocidal activity in the range of concentrations assayed (data not shown). To test whether the derivatives would display any *in vitro* activity against the intracellular forms of *T. cruzi*, $1 \mu\text{g mL}^{-1}$ of each compound was assayed as previously stated [22], with Fig. 2 showing that Allop as well as the **2a**, **2b** and **3c**, derivatives inhibited *T. cruzi* amastigotes (AMAS) growth in a better, or at least similar way to Bz.

In order to estimate their IC₅₀ values, *T. cruzi* infected cell monolayers were subjected to 0.5–50 μM of each derivative and the percentage of infection was calculated. As can be seen in Fig. 3a, only the Allop and **3c** compounds were able to reduce the proliferation of intracellular AMAS of virulent RA strain in Vero cells [23],

with the load of AMAS in cell monolayers being reduced by treatment with 5 or 50 μM of each drug ($p < 0.001$) (Fig. 3b). Both the Allop and **3c** compounds displayed a dose-dependent trypanocidal effect, showing IC₅₀ values of 9.62 and 11.30 μM , respectively.

Neither Allop nor the **3c** derivatives were toxic for mammalian cells at the concentration tested (Fig. 4).

2.3. Physicochemical properties

2.3.1. Acid dissociation constants (pKa)

There are different experimental and theoretical methods for determining the pKa [24], with software packages usually being employed to estimate this parameter. Meloun and Bordovská [25] evaluated the accuracy of the pKa data generated by Advanced Chemistry Design (ACDpKa) packages, and concluded that this software provided the most accurate pKa prediction. In order to validate this theoretical method, we obtained the pH-solubility profile of Allop (data not shown), which gave a pKa value of 9.7, being similar to that obtained by ACDpKa software. All these values are reported in Table 1.

Although the Allop drug molecule has two acidic groups, for all the derivatives studied only the ionization of the NH-5 atom was observed, with compounds **2a–c** showing similar pKa values (pKa 9.3) to Allop (pKa 9.7). However, compounds **3a–c** presented lower pKa values than the parent compound (pKa 7.6), due to the $-\text{C}(\text{O})-\text{R}$ substituent in the N – 1 atom providing more acidic characteristics to the molecules. The pKa values of **3a–c** are in agreement with those reported by Bundgaard and Falch [20].

2.3.2. Integrity

Stability indicating methods have become an important aspect of Food and Drug Administration (FDA) requirements. In addition, there is an increasing tendency toward the development of stability indicating assays, using the approach of stress testing as mentioned in the International Conference on Harmonisation (ICH, guidelines Q1A) [26] and Guidance for Industry of FDA [27] concerning an *in vivo* bioavailability that included a discussion on gastrointestinal (GI) stability. Another important aspect to consider is the stability of drug molecules in plasma, which provides useful information for *in vivo* studies and potential structural modifications.

Stress testing also encompasses the influence of, among others, oxidizing agents, light, temperature and susceptibility over a wide range of pH values. In contrast, the FDA has recommended stability studies of 1 h in simulated gastric fluid (SGF; pH 1.2 with pepsin) and 3 h in simulated intestinal fluid (SIF; pH 6.8 with pancreatin) in order to mimic GI conditions. Thus, a significant degradation (>5%) of a drug molecule could suggest potential instability in the gastrointestinal tract (GIT) [27]. For this reason, the aim of the current study was also to determine the inherent stability of **2a–c** and **3a–c** under these conditions, using a validated Micellar Liquid Chromatography (MLC) as the analytical method.

2.3.2.1. *Validation method.* The FDA guidelines [28] were followed to validate the MLC method, by evaluating linearity, limit of detection, limit of quantification, intra and inter-day precision, selectivity and recovery parameters. This method was validated for all compounds according to their chemical structures; Method A for **2a–c** and Method B for **3a–c** (see Experimental section). Fig. 5a,b shows chromatograms obtained from a mixture of **2a–c** and **3a–c** in their respective matrices, showing that there was no interference between Allop and their derivatives. These results revealed that **2a–c** and **3a–c** could be quantified by MLC in the presence of Allop as a degradation product.

2.3.2.1.1. *Calibration parameters, limit of detection (LOD) and limit of quantification (LOQ).* The calibration graphs for all

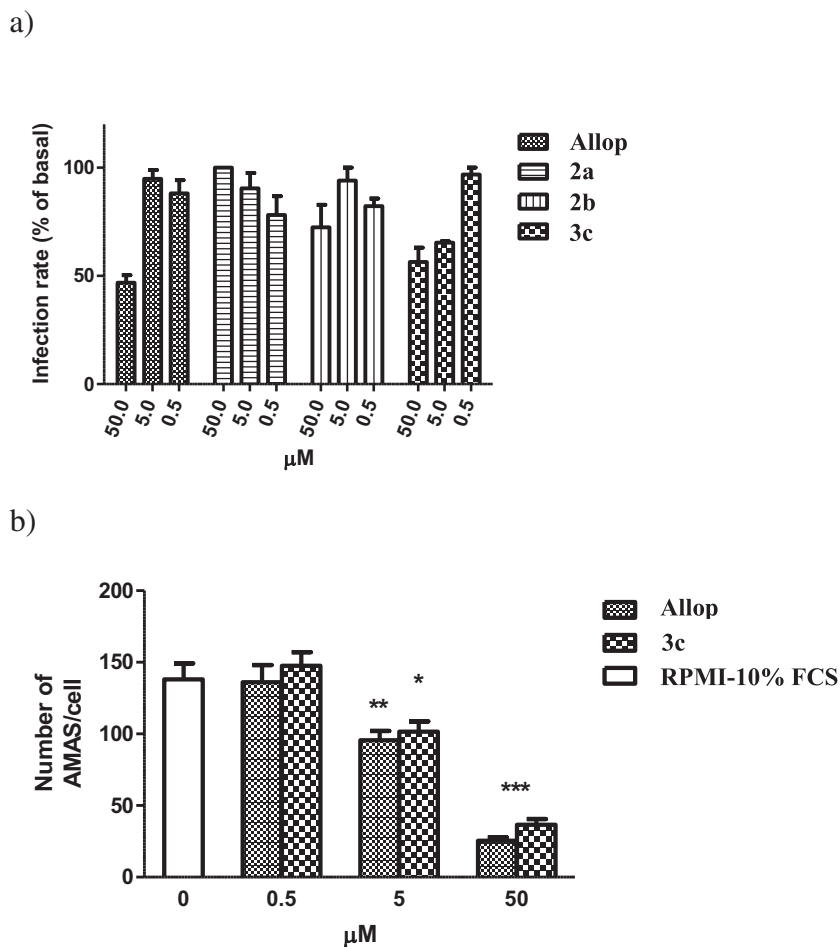


Fig. 3. Effect of **2a**, **2b** and **3c** derivatives of Allopurinol on the growth of *T. cruzi* amastigotes. AMAS were cultured in triplicate in the presence of 0.5–50 μM of each compound. a) The rate of infection was determined as the percentage of the treated *T. cruzi*-infected cells over the basal untreated *T. cruzi*-infected cells. b) The number of AMAS/cell was counted over a total of 100 infected cells, as described in [Experimental section](#). Results are expressed as means ± SE from three independent experiments. **p* < 0.05; ***p* < 0.01; ****p* < 0.001 from the Bonferroni post-test.

compounds were constructed using the areas of the chromatographic peaks (triplicate injections) obtained at seven different concentrations equally distributed in the range 5×10^{-9} to 5×10^{-7} mol mL⁻¹. The adjusted parameters obtained are shown in

[Table 1S](#), and the regression coefficients (*r*²) were always higher than 0.9998.

The LOD for Allop, **2a–c** and **3a–c** was calculated using the *3s criterion* (three times the standard deviation of the lowest concentration solution included in the calibration divided by the slope of the calibration graph) for a series of 10 solutions containing low concentrations of each compound ([Table 1S](#)). The LOQ was then

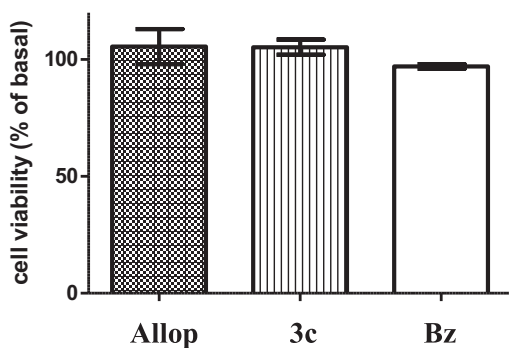


Fig. 4. Effect of **3c** derivative on murine splenocyte viability. Cultures were carried out on 96-well plates with 2×10^6 cells mL⁻¹ for 32 h in the presence of compound **3c** at a concentration of $50 \times$ IC₅₀. Cell viability was determined by the Alamar Blue™ method according to the instructions of the manufacturer. Data are expressed as the percentage of viability compared to control (non-treated cells). Bz and Allop were considered as reference drugs. Bars represent the means ± SE of two experiments carried out in duplicate.

Table 1

Acid dissociation constants (pKa), intrinsic solubility (*S*₀) and melting point (mp, °C) of Allop and its derivatives.

Comp	pKa	<i>S</i> ₀		mp
		25 °C	37 °C	
Allop	9.7 ^a ; 9.3 ± (0.4) ^b	0.49 ± (0.05) ^d	0.90 ± (0.04) ^d	>350
2a	9.3 ± (0.4) ^b	1.48 ± (0.10) ^d	2.02 ± (0.30) ^d	304
2b	9.3 ± (0.4) ^b	0.71 ± (0.06) ^d	0.94 ± (0.03) ^d	325
2c	9.3 ± (0.4) ^b	2.07 ± (0.05) ^d	2.56 ± (0.15) ^d	292
3a	7.6 ± (0.4) ^{b,c} ; 7.7 ^c	>65 ^e	>65 ^e	267
3b	7.6 ± (0.4) ^{b,c}	>65 ^e	>65 ^e	275
3c	7.6 ± (0.4) ^{b,c}	>65 ^e	>65 ^e	233

^a Calculated from the pH-solubility profile (25 °C).

^b ACDpKa.

^c Bundgaard et al.

^d mg mL⁻¹.

^e μg mL⁻¹.

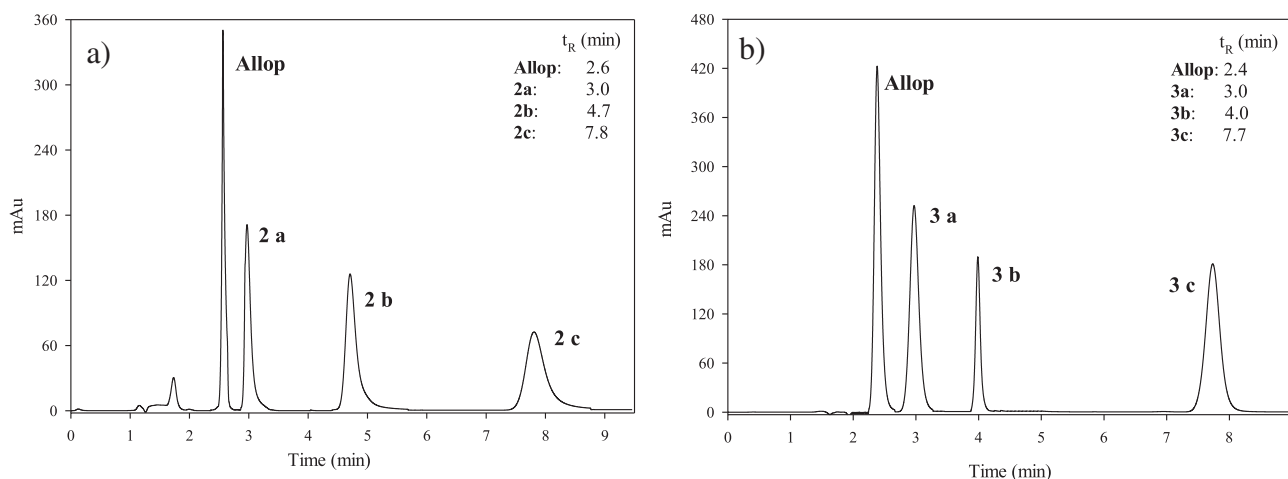


Fig. 5. MLC chromatograms showing: (a) Allop and **2a–c** derivatives in simulated intestinal fluid, (b) Allop and **3a–c** derivatives in simulated gastric fluid. For details of the chromatographic conditions, see Section 4.5.

selected for the lowest concentrations used in the calibration graphs.

2.3.2.1.2. Recovery and precision (intra- and inter-day). For the recovery assays, three different concentrations ($c_1 = 7.5 \times 10^{-9}$, $c_2 = 6 \times 10^{-8}$ and $c_3 = 3.5 \times 10^{-7}$ mol mL⁻¹, ten replicates for each standard) for all compounds were spiked in the buffers (pH 1.2 and pH 6.8) and in the SGF and SIF matrices, and then analyzed in the proposed mobile phases for each series of compounds. The standard solutions were processed and analyzed following the above-described procedure and relative (analytical) recovery was calculated by comparing the obtained concentration from the standard solutions with those of the working ones. Table 2S lists an average of the percentage of recovery in all matrices, which revealed satisfactory recoveries and no significant deviations for all the studied compounds.

The intra- and inter-day precisions were determined by analyzing all compounds at the same concentrations of the recovery. The intra-day precision was evaluated by injecting these three test solutions ten times on the same day whereas the inter-day precision determination involved calculating the average of ten

measurements of the intra-day precision values taken on ten days over a 3-month period, performed by different analysts and using various apparatus at the same concentrations. In Table 3S, the results of intra- and inter-day precisions are expressed as the percentage of the relative standard deviation (RSD, %) for the intra- and inter-day values. In all cases, the RSD values were lower than 1.85%.

These results showed that the proposed MLC method was suitable for the analysis of these compounds in buffer solutions and also in the SGF and SIF samples. Therefore, the procedure developed here can be used for the quality control, routine analyses and pharmacokinetic studies of all the Allop derivatives.

2.3.2.2. Degradation studies of Allop derivatives: hydrolytic, oxidative and buffer solutions (pH 1.2 and pH 6.8), SGF, SIF and human plasma. The accelerated degradation studies for the six derivatives of Allop were assayed under the ICH and FDA recommendation procedures in order to identify their degradation products. In all cases, however, only Allop was detected. Table 2 shows the percentages of degradation (%), $t_{1/2}$ and kinetic constants (k_{obs} , where appropriate) for Allop, **2a–c** and **3a–c** compounds under-hydrolytic and oxidative conditions as well as in buffers (pH 1.2 and 6.8), SGF, SIF and human plasma matrices.

Under stress conditions, only up to 10% of the degradation process was observed for derivatives **2a–c** in NaOH (0.1 M) at 90 °C after 16 h (3.7–10.4%), whereas for **3a–c** an immediate degradation took place not only in NaOH (0.1 M) but also in the HCl (0.1 M) and H₂O₂ (3.5%) solutions. Although, under FDA conditions, the **2a–c** derivative was stable in all media, **3a–c** suggested instability in the GIT. For **3a–c** in SGF and pH 1.2, up to 32% of degradation was observed during 1 h, with no significant differences observed in their k_{obs} for pepsin action. In contrast, in SIF and pH 6.8 conditions, the **3a–c** derivatives underwent a 100% degradation after 3 h of reaction, and pancreatin may have been responsible for this process. In human plasma, Allop and **2a–c** were stable at 100%, while the **3a–c** derivatives were very unstable and interacted in all the stability studies. It was also observed that all compounds followed a pseudo-first-order degradation kinetics.

These results show that Allop was stable for all matrices and studied conditions, indicating that C6-derivatives acted as drugs whereas the N1-ones behaved as prodrugs and yielded Allop in a short time period under physiological conditions, but immediately under stress conditions.

Table 2

Stability studies of Allop and its derivatives in sodium hydroxide (NaOH, 0.1 M, 90 °C), hydrochloric acid (HCl, 0.1 M, 90 °C), hydrogen peroxide (H₂O₂) 30% for **2a–c** and 3.5% for **3a–c**, simulated gastric and intestinal fluids (SGF, SIF, respectively), buffers pH 1.2 and 6.8, and human plasma.

Comp	Stress conditions			FDA conditions			Human plasma
	NaOH	HCl	H ₂ O ₂	SGF	pH 1.2	SIF	
Allop	No degradation						
2a	10.4 ^a	No degradation					
2b	9.3 ^a						
2c	3.7 ^a						
3a	Immediate degradation	18.9 ^b	17.1 ^b	100 ^c	100 ^c	0.0052 ^d	0.0051 ^d
3b		32 ^b	30.3 ^b	100 ^c	100 ^c	0.0074 ^d	0.0071 ^d
3c		26.5 ^b	27.0 ^b	100 ^c	100 ^c	0.0380 ^d	0.0380 ^d
		0.0062 ^d	0.0063 ^d	0.0455 ^d	0.0299 ^d	0.0186 ^d	0.0186 ^d

^a % degradation (16 h).

^b % degradation (37 °C, 1 h).

^c % degradation (37 °C, 3 h).

^d k_{obs} min⁻¹.

^e $t_{1/2}$ (min).

2.3.3. Solubility

Many protocols have been described in the literature for measuring solubility, with classical approaches being based on the saturation shake-flask method [29,30], which was used to determine the intrinsic solubility equilibrium constant, S_0 , of Allopol and **2a–c**, in the buffer pH 6.8 at 25 °C (of interest in pharmaceutical operations) and at 37 °C. These experimental solubility data are shown in Table 1, with the Allopol value being similar to that of literature [31].

Taking into account that the **3a–c** derivatives can degrade over the time of the study, we used the turbidity detection, which was popularized by Lipinski et al. [21]. In all cases, the solubility in buffer pH 6.8 at 25 °C and 37 °C was greater than 65 $\mu\text{g mL}^{-1}$, suggesting that the solubility was not responsible for the poor bioavailability of these compounds [21].

Taking into account that the melting point of solids is an indicator of molecular cohesion, it can be used as a guide to the solubility value in a closely related series of compounds. [32]. Therefore, as we observed that **2a–c** and **3a–c** melted at lower temperatures than Allopol (Table 1) accompanied by decomposition-volatizing processes, this may indicate a lower lattice energy that might also be associated with the improved solubility of the Allopol derivatives [32].

2.3.4. Lipophilicity

Although the octanol–water distribution ratio, $P_{o/w}$, is generally accepted to be the best physicochemical property to measure the hydrophobicity of chemicals, it has been demonstrated that the capacity factor (k') of a compound obtained by RP-HPLC is an indirect reliable descriptor of its lipophilicity. Moreover, the $\log k'_w$ (an extrapolated parameter from the binary phase to 100% of water, and is an even better descriptor of lipophilicity because it is independent of any organic modifier effects [33].

Here, we used the method proposed by the Organization for Economic Cooperation and Development (OECD), who prepared guidelines that should be followed in order to produce reliable $P_{o/w}$ values using RP-HPLC [34]. According to OECD, the $\log P_{o/w}$ value of an analyte can be evaluated from a calibration graph constructed from the $\log P_{o/w}$ values of literature versus experimental $\log k'_w$ of reference compounds. In this way, seven compounds (Allopol [31], didanosine [35], aniline [34], phenol [34], benzoic acid [34], toluene [34] and naphthalene [34]) were used as standard compounds, and the following good correlation was found (eq. (1)) between $\log k'_w$ and the $\log P_{o/w}$ values of the reference compounds.

$$\log P_{o/w} = 1.348 \pm (0.106)\log k'_w - 0.011 \pm (0.028) \quad (1)$$

$n = 7; r^2 = 0.9953; \text{SD} = 0.280$

Table 3
Molecular properties of Allopol and its derivatives.

Comp	Lipinski rules (LR)				PSA ^a	NRB ^b
	Lipophilicity (Log P_{ow})	H-bond donor	H-bond acceptors	MW		
Allopol	−0.55	2	3	136.1	74.4	0
2a	−0.05	2	3	150.1	74.4	0
2b	0.52	2	3	164.2	74.4	1
2c	1.14	2	3	178.2	74.4	2
3a	0.40	1	5	178.2	80.6	0
3b	1.22	1	5	192.2	80.6	1
3c	1.99	1	5	206.2	80.6	2
OP^c	<5	≤5	≤10	<500	≤140	≤10

^a Polar surface area (PSA).

^b Number of rotatable bonds (NRB).

^c Optimal properties for bioavailability and oral absorption (OP).

This equation may be regarded as a special case of the Collander one, which relates the partition coefficients measured in two different partitioning systems. In fact, the slope of the Collander equation is a measure of the solvent system's sensitivity to changes in the hydrophobicity of the solutes relative to n-octanol, (i.e a slope of 1.0 indicates isodiscriminative behavior). Eq. (1) has a slope of 1.35, thus indicating a good system study [36]. The $\log k'_w$ values of compounds **2a–c** and **3a–c** were then used to determine their $\log P_{o/w}$ values from this standard curve with Table 3 showing these obtained values and Fig. 6 demonstrating the correlation between the standard curve and the analyzed derivatives.

It is important to point out that Bundgaard et al reported $\log P_{o/w}$ values in pure water (pH \cong 6.5) for N1-derivatives of −0.35; 0.30 and 0.85 (acetyl-, n-propyl- and n-butyl-, respectively) [20]. In this medium, these compounds were partially ionized (pKa = 7.6) whereas in our study (buffer pH 5.5) they behaved as unionized ones. For this reason, the $\log P$ values reported by Bundgaard seemed to be more hydrophilic than those we obtained here ($\log P = 0.40, 1.22$ and 1.99 , for **3a**, **3b** and **3c**, respectively).

2.3.5. Other relevant properties

For the majority of drugs, the preferred route of administration is by oral ingestion, and therefore when considering the potential pharmacological use of **2a–c** and **3a–c**, they must demonstrate an adequate *in vivo* behavior. The “rule of five”, developed by Lipinski et al. [21] [$\log P < 5$, H-bond donor ≤ 5 (expressed as the sum of OH and NH groups), H-bond acceptor ≤ 10 (expressed as the sum of N and O atoms), and molecular weight < 500] is the most widely accepted method used. In recent years, this rule has been expanded to the study of other parameters, such as polar surface area (PSA) and molecular rigidity as indicated by the number of rotatable bonds (NRB) [37]. Considering that Lipinski thought that certain properties were important for drug bioavailability and absorption, if two of these parameters are out of range, a poor absorption or permeability is possible.

The PSA, defined as the sum of surfaces of polar atoms in a molecule, provides a good correlation with experimental transport data. This has been successfully applied for the prediction of intestinal absorption, among other parameters [38], with the physical explanation being that polar groups are involved in the desolvation process when they move from an aqueous extracellular environment to the more lipophilic interior of the membranes. In addition, it has been shown that PSA, calculated according to the method proposed by Ertl et al. [39], in most cases produces a sigmoid relationship with intestinal absorption, showing that poorly

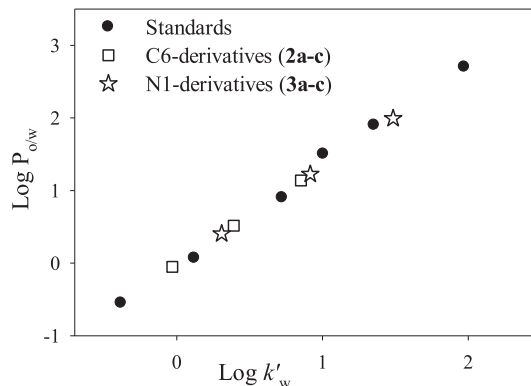


Fig. 6. Relationship between $\log k'_w$ and $\log P_{o/w}$ values for standards and Allopol derivatives.

absorbed compounds are identified as those with $PSA \geq 140 \text{ \AA}^2$ [38].

The last parameter studied was the molecular rigidity, which suggests that if NRB is >10 a poor oral bioavailability could occur [37]. Summing up, when the developed derivatives **2a–c** and **3a–c** were subjected to Lipinski rules, PSA and NRB analyses, it can be observed in Table 3, that all of them exhibited acceptable characteristics.

3. Conclusions

Different strategies were developed for the synthesis of six Allop derivatives (**2a–c** and **3a–c**), which were unequivocally characterized by different spectroscopic methods. Regarding these analyses, the results showed that all derivatives had a better physicochemical profile than Allop, as well as that all met Lipinski's rules and had suitable characteristics of PSA and NRB.

When the inhibitory effects of the C6-alkyl- and N1-acyl derivatives of Allop against *T. cruzi* were studied, none of the compounds showed any significant trypanocidal activity *in vitro* against TRYP. In contrast, the AMAS resulted susceptible to the **2a**, **2b** and **3c** derivatives of Allop when tested at $1 \mu\text{g mL}^{-1}$. As this hypoxanthine analog is used by the *T. cruzi*'s HGPRT as an alternative substrate during the duplicative process [10], it is certain that the AMAS forms were involved. On testing different concentrations of the derivatives, only the **3c** compound displayed an inhibitory effect, probably by being incorporated into the parasite ribonucleic acid as no physiological nucleotides or blocking of the synthesis of new purine nucleotide occurred. The **3c** derivative exhibited an IC50 value similar to Allop, which was not toxic for mammalian cells. The development and maintenance of chronic lesions are due to persistent intracellular parasites in targeted tissues, which the immune response is unable to eradicate.

Hence, the possible role of **3c** in Chagas disease may become a practical tool in the improvement of the prognosis of these patients. It is important to point out that modifications on C-6 (**2a–c**) led to chemical entities that could not be transformed into Allop in biological media such as plasma and SIF. Although these compounds did not have parasitocidal activity *per se*, they presented better physicochemical properties than the prototype (Allop).

The **3a–c** series were promising candidates, especially compound **3c**, since it demonstrated not only excellent activity against *T. cruzi*, but also no cytotoxicity and gave Allop in an adequate time. These features led to a better lipophilicity and solubility than Allop, as well as to a lower crystalline lattice, with the possibility of better pharmacokinetic profiles of the regenerated active compound.

4. Experimental section

4.1. Chemicals and reagents

Allopurinol, propionic anhydride, butyric anhydride, acetyl chloride, propionyl chloride and butyryl chloride were purchased from Sigma, and acetic anhydride was purchased from Merck. The buffer materials of pH 1.2 (hydrochloric acid/sodium chloride), pH 5.5 (acetic acid/sodium acetate) and pH 6.8 (sodium dihydrogen phosphate/phosphoric acid) were of analytical reagent grade.

The SGF and SIF were prepared according to USP specifications [40]. Sodium dodecyl sulfate (SDS) was purchased from Biopack, 1-propanol (analytical grade) was purchased from Cicarelli and methanol (MeOH, HPLC grade) was acquired from Sintorgan. The water used in all studies was of Milli-Q grade (Millipore®), and solutions and mobile phases were filtered through Millipore filters Type FH (4.5 μm) (Millipore) and degassed under vacuum. Reagents

were of commercial quality ($>97\%$) from freshly opened containers, and solvents were of analytical grade.

4.2. Equipment

High Resolution Mass Spectrometry (HRMS) was performed in a Bruker micrOTOF-Q II, using the electrospray ionization (ESI) positive mode and atmospheric pressure photoionization (APPI). Nuclear Magnetic Resonance (NMR) experiments were performed on Bruker Avance II 400, Ultrashield, Frequency ^1H NMR 400.16 MHz and ^{13}C NMR 100.62 Hz, Dual BBI Probe, at 25°C , using DMSO- d_6 (99.8%, Merck) as solvent. The assignment of all exchangeable protons (OH, NH) was confirmed by the addition of D_2O (99.9%, Sigma), and chemical shift values are reported in parts per million (δ) relative to tetramethylsilane (TMS). The splitting pattern abbreviations are as follows: s, singlet; d, doublet; t, triplet; qua, quartet; quin, quintet. Ultraviolet spectrophotometric (UV) studies were carried out using a Shimadzu Model UV-160A spectrophotometer, with 1 cm quartz cells. Melting point (mp) and thermal analysis were carried out using differential scanning calorimetry (DSC) 2920 modulated DSC (TA Instrument); the temperature axis and the cell constant of the DSC were calibrated with indium, and thermogravimetric analysis (TG) measurements were performed with a TA Instrument Hi-res TG 2950 (TA Instrument). Weighed samples (1.5–3 mg, C-33 Microbalance, Cahan) were scanned in covered aluminum (Al) pans under a dynamic dry nitrogen atmosphere (50 mL min^{-1}). The pH values were measured with a CRI-SON GLP-21 pH meter equipped with an Ag/AgCl glass electrode.

4.3. Chemistry

4.3.1. Characterization of C6-alkyl series (**2a–c**)

4.3.1.1. *6-Methyl-1,5-dihydro-4H-pyrazolo[3,4-d]pyrimidin-4-one (2a)*. Light yellow solid (82% yield), $R_f = 0.45$ ($\text{CH}_2\text{Cl}_2/\text{EtOH}$ 10:1); mp: 304°C ; HPLC tr = 3.7 min, MLC tr = 3.0 min. ^1H NMR (DMSO- d_6): δ 13.55 (s, 1H, NH-1), 11.92 (s, 1H, NH-5), 8.00 (s, 1H, H-3), 2.33 (s, 3H, H-1'). ^{13}C NMR (DMSO- d_6): δ 159.3 (CO, C-4), 157.5 (C, C-6), 155.8 (C, C-7a), 134.2 (CH, C-3), 104.1 (C, C-3a), 21.9 (CH_3 , C-1'). HRMS (APPI) calcd for $\text{C}_6\text{H}_7\text{N}_4\text{O}$ ($\text{M} + \text{H}^+$) m/z : 151.0614; found: 151.0622; UV $\lambda_{\text{max}}/\text{nm}$ (MeOH, pH 5) 250.

4.3.1.2. *6-Ethyl-1,5-dihydro-4H-pyrazolo[3,4-d]pyrimidin-4-one (2b)*. Light yellow solid (83% yield): $R_f = 0.64$ ($\text{CH}_2\text{Cl}_2/\text{EtOH}$ 10:1); mp: 325°C ; HPLC tr = 5.3 min, MLC tr = 4.7 min. ^1H NMR (DMSO- d_6): δ 13.58 (s, 1H, NH-1), 11.92 (s, 1H, NH-5), 7.98 (s, 1H, H-3), 2.63 (qua, 2H, H-1'), 1.22 (t, 3H, H-2'). ^{13}C NMR (DMSO- d_6): δ 162.1 (C, C-6), 158.8 (CO, C-4), 154.7 (C, C-7a), 135.4 (CH, C-3), 104.1 (C, C-3a), 28.0 (CH_2 , C-1'), 11.7 (CH_3 , C-2'). HRMS (APPI) calcd for $\text{C}_7\text{H}_9\text{N}_4\text{O}$ ($\text{M} + \text{H}^+$) m/z : 165.0771; found: 165.0778. UV $\lambda_{\text{max}}/\text{nm}$ (MeOH, pH 5) 250.

4.3.1.3. *6-Propyl-1,5-dihydro-4H-pyrazolo[3,4-d]pyrimidin-4-one (2c)*. Light yellow solid (81% yield): $R_f = 0.72$ ($\text{CH}_2\text{Cl}_2/\text{EtOH}$ 10:1); mp: 292°C ; HPLC tr = 8.8 min, MLC tr = 7.8 min. ^1H NMR (DMSO- d_6): δ 13.55 (s, 1H, NH-1), 11.98 (s, 1H, NH-5), 7.99 (s, 1H, H-3), 2.57 (t, 2H, H-1'), 1.71 (sex, 2H, H-2'), 0.91 (t, 3H, H-3'). ^{13}C NMR (DMSO- d_6): δ 160.5 (C, C-6), 159.3 (CO, C-4), 155.6 (C, C-7a), 134.2 (CH, C-3), 104.2 (C, C-3a), 36.5 (CH_2 , C-1'), 20.7 (CH_2 , C-2'), 14.0 (CH_3 , C-3'). HRMS (APPI) calcd for $\text{C}_8\text{H}_{11}\text{N}_4\text{O}$ ($\text{M} + \text{H}^+$) m/z : 179.0927; found: 179.0938. UV $\lambda_{\text{max}}/\text{nm}$ (MeOH, pH 5) 250.

4.3.2. Characterization of N1-acyl series (**3a–c**)

4.3.2.1. *1-Acetyl-1,5-dihydro-4H-pyrazolo[3,4-d]pyrimidin-4-one (3a)*. White solid, recrystallization from DMF/EtOH (60% yield); $R_f = 0.73$ ($\text{CH}_2\text{Cl}_2/\text{EtOH}$ 8:2); mp: 267°C ; HPLC tr = 3.7 min, MLC

tr = 3.0 min. ^1H NMR (DMSO- d_6): δ 12.74 (s, 1H, NH-5), 8.36 (s, 1H, H-3), 8.28 (d, 1H, H-6), 2.73 (s, 3H, H-2'). ^{13}C NMR (DMSO- d_6): δ 168.9 (CO, C-1'), 157.4 (CO, C-4), 154.9 (C, C-7a), 150.7 (C, C-6), 138.5 (CH, C-3), 109.3 (C, C-3a), 24.6 (CH₃, C-2'). HRMS (ESI) calcd for C₇H₆N₄NaO₂ (M + Na)⁺ *m/z*: 201.0383; found: 201.0394. UV λ_{max} /nm (MeOH, pH 5) 276.

4.3.2.2. 1-Propanoyl-1,5-dihydro-4H-pyrazolo[3,4-d]pyrimidin-4-one (3b). White solid, recrystallization from DMF/EtOH (62% yield), *R_f* = 0.77 (CH₂Cl₂/EtOH 8:2); mp: 275 °C; HPLC tr = 4.9 min, MLC tr = 4.0 min. ^1H NMR (DMSO- d_6): δ 12.72 (s, 1H, NH-5), 8.35 (s, 1H, H-3), 8.28 (d, 1H, H-6), 3.21 (qua, 2H, H-2'), 1.17 (t, 3H, H-3'). ^{13}C NMR (DMSO- d_6): δ 172.5 (CO, C-1'), 157.3 (CO, C-4), 154.9 (C, C-7a), 150.7 (C, C-6), 138.4 (CH, C-3), 109.2 (C, C-3a), 29.8 (CH₂, C-2'), 8.8 (CH₃, C-3'). HRMS (ESI) calcd for C₈H₈N₄NaO₂ (M + Na)⁺ *m/z*: 215.0539; found: 215.0655. UV λ_{max} /nm (MeOH, pH 5) 276.

4.3.2.3. 1-Butanoyl-1,5-dihydro-4H-pyrazolo[3,4-d]pyrimidin-4-one (3c). White solid, recrystallization from EtOH (65% yield), *R_f* = 0.82 (CH₂Cl₂/EtOH 8:2); mp: 233 °C; HPLC tr = 7.0 min, MLC tr = 7.7 min. ^1H NMR (DMSO- d_6): δ 12.71 (s, 1H, NH-5), 8.35 (s, 1H, H-3), 8.28 (s, 1H, H-6), 3.18 (t, 2H, H-2'), 1.71 (sex, 2H, H-3'), 0.97 (t, 3H, H-4'). ^{13}C NMR (DMSO- d_6): δ 171.6 (CO, C-1'), 157.6 (CO, C-4), 155.1 (C, C-7a), 150.8 (C, C-6), 138.7 (CH, C-3), 109.5 (C, C-3a), 38.2 (CH₂, C-2'), 17.8 (CH₂, C-3'), 14.1 (CH₃, C-4'). HRMS (ESI) calcd for C₉H₁₀N₄NaO₂ (M + Na)⁺ *m/z*: 229.0696; found: 229.0711. UV λ_{max} /nm (MeOH, pH 5) 276.

4.4. Activity

4.4.1. Parasites

Bloodstream trypomastigotes (TRYP) of RA strain of *T. cruzi* [23] were obtained from *T. cruzi* infected mice at the peak of parasitemia. To enrich blood supernatants with TRYP, PBS-diluted blood was centrifuged, incubated for 1 h at 37 °C and the supernatant was collected. Thus, parasites were pelleted by centrifugation for 30 min at 10,000 × *g*, counted in a Neubauer hemacytometer and diluted to 1.5 × 10⁶ TRYP mL⁻¹ in RPMI 1640 medium supplemented with 10% fetal calf serum (FCS) for drug sensitivity assays.

4.4.2. In vitro drug activity against bloodstream trypomastigotes

Purified TRYP were incubated under an atmosphere of 5% CO₂ at 37 °C for 24 h with increasing doses of each synthetic compound (0–70 μg mL⁻¹) obtained from stock solutions of 40 mM dissolved in DMSO. Benznidazole was considered as the reference drug. The final concentration of DMSO in the culture medium remained below 0.5%. A solution of 0.5% DMSO was used as negative control. The following day, the remaining live parasites were counted using a Neubauer chamber as previously described [41]. Three independent experiments were performed in triplicate.

4.4.3. In vitro drug activity against intracellular amastigotes

Irradiated Vero cells (2000 rads) seeded on round coverslips were infected with TRYP. After 24 h of parasite–host cell interaction (5:1 parasite:cell ratio), the infected cultures were washed to remove free parasites and incubated for another 72 h with 1 μg mL⁻¹ of each compound, as previously described [22]. Cell cultures were maintained at 37 °C in 5% CO₂. Uninfected treated cultures exposed to vehicle (0.5% DMSO) were used as controls. The method for determining the rate of infection of host cells by *T. cruzi* has previously been described in detail [42]. Briefly, host cells, attached to the coverslip seeded in a 24-well plate, were gently rinsed with PBS before being air dried, fixed in absolute methanol and stained with Giemsa. The coverslip was then transferred to a glass slide and the mounted cells were observed under a light

microscope. The percentage of host cells with more than one amastigote (AMAS) in their cytoplasm was calculated by analyzing a total of 400 host cells distributed in randomly chosen microscopic fields. Data expressed as the percentage of inhibition of each compound were compared with non-treated cells. Only those drugs that displayed a similar or better behavior than Bz were used for the IC₅₀ calculation. In this case, *T. cruzi* infected monolayers were subjected to 0.5–50 μM of selected compounds, and the rate of infection as well as the mean number of AMAS per infected cell was determined. The 50% inhibitory concentrations (IC₅₀s) were estimated by nonlinear regression analysis using Graph Pad Prism 5.03 software (La Jolla, USA).

4.4.4. Mammalian cell toxicity assays

Only those compounds that attained an IC₅₀ index in mammalian cells 50 times greater than the IC₅₀ of the parasite were considered for further *in vivo* evaluation. Cultures were carried out on 96-well plates with 2 × 10⁶ murine splenocytes mL⁻¹ for 32 h in the presence of compound **3c**, Bz and Allopat at a concentration of 50 × IC₅₀. Cell viability was determined by the Alamar Blue™ method according to instructions of the manufacturer. Data were expressed as the percentage of viability related to control (non-treated cells). An analysis of variance (ANOVA) with the Bonferroni post-test was used to carry out the statistical analysis. A *p* value < 0.05 was considered significant.

4.5. Chromatographic conditions

Analytical thin layer chromatography (TLC) was performed on percolated plates purchased from Merck (Silica Gel 60 F254). Solvent system: **2a–c**: CH₂Cl₂/EtOH 10:1; **3a–c**: CH₂Cl₂/EtOH 8:2. HPLC and MLC analyses were carried out using an Agilent® 1100 apparatus equipped with a Phenomenex® column, Hypersil ODS 5 μ particle diameter (4.6 × 250 mm); HPLC conditions: **2a–c**: 80% 0.01 M NaC₂H₃O₂/CH₃COOH (pH 4.5), 20% MeOH, flow rate of 1.5 mL min⁻¹, 35 °C, λ = 250 nm; **3a–c**: 50% buffer pH 4.5 (NaC₂H₃O₂/CH₃COOH), 50% MeOH, flow rate of 1 mL min⁻¹, 35 °C, λ = 276 nm; MLC conditions: **2a–c**: SDS (0.05 M) – NaH₂PO₄/H₃PO₄ (0.01 M, pH 3.0), flow rate of 1.25 mL min⁻¹, 25 °C, λ = 250 nm; **3a–c**: SDS (0.1 M) – 7.5% (v/v) 1-propanol – NaH₂PO₄/H₃PO₄ (0.01 M, pH 3.0), flow rate of 1 mL min⁻¹, 25 °C, λ = 276 nm.

4.6. Stability studies

4.6.1. Hydrolytic and oxidative studies

Compounds **2a–c** and **3a–c** at a concentration of 1 mg mL⁻¹ were used in all stability assays. Acid and alkaline decomposition studies were performed by heating the solution of each compound in 0.1 M HCl or 0.1 M NaOH at 90 °C for 16 h.

4.6.2. Buffers (pH 1.2 and pH 6.8), SGF, SIF and human plasma

The stock solutions (1.0 × 10⁻⁴ mol mL⁻¹) of each compound were prepared in DMSO prior to use. Then, 100 μL of the stock solution were added to a vial containing 1900 μL of buffer or matrix (gastric or intestinal fluid) to obtain the work solutions. Afterward, the vials containing the samples were placed in a water bath at 37 °C throughout the experiment. In human plasma, the experiments were performed under the experimental conditions suggested by Di et al. [43]. Human plasma (unit N° 65261) was generously supplied by Instituto de Hematología, Hemoterapia y Banco de Sangre, Universidad Nacional de Córdoba, Argentina.

4.6.3. Chromatographic analysis

At an appropriate time, aliquots of 100 μL were removed and then centrifugated. Then, 50 μL of the resulting supernatant was

added to a solution of 450 μL of the corresponding mobile phase. Each sample was immediately stored at $-18\text{ }^{\circ}\text{C}$ until use. Upon removal of the last samples, the stored solutions were allowed to warm up to room temperature, and then the concentrations of **2a–c** and **3a–c** from the work solutions were monitored by MLC to determine the rate at which the parent compounds disappeared, with the formation of AlloP being the only degradation product.

4.7. Solubility

The solid compounds AlloP and **2a–c** were added to a standard phosphate buffer solution (pH 7.0, 80 mM) until saturation occurred as indicated by undissolved excess drug. The thermostated saturated solution ($25\text{ }^{\circ}\text{C}$) was shaken for 24 h to produce an equilibrium between the two phases. At different times, the aliquots were removed and then centrifugated. The resulting supernatant was analyzed by MLC to determine the integrity and concentration of each compound.

For **3a–c**, the stock solutions ($10\text{ }\mu\text{g }\mu\text{L}^{-1}$) of each compound were prepared in DMSO, and $1\text{ }\mu\text{L}$ of the corresponding solutions was added into a cuvette containing 2.5 mL pH 7.0 phosphate buffer, with these steps being repeated up to 14 times. After each step, an equilibrium time of 2 min was allowed before the turbidity was analyzed. The precipitated particles led to an increase in UV absorbance (600–800 nm) due to light scattering. The system was kept under stirring at a controlled temperature of $25\text{ }^{\circ}\text{C}$.

4.8. Determination of lipophilicity by RP-HPLC ($\log k'_{ow}$)

The instrument conditions for all the analyses were as follows: $25\text{ }^{\circ}\text{C}$, flow rate: 1 mL min^{-1} , injection volume: $20\text{ }\mu\text{L}$. Each analysis was performed isocratically using buffer pH 5.5–MeOH with a methanol content of between 30% and 75% (v/v) at 5% increments. Three injections were performed for each compound and five injections for the standards at each MeOH–buffer ratio. The logarithm of the capacity factor ($\log k'$) for **2a–c**, **3a–c** and the standard compounds was calculated for each MeOH–buffer ratio from the retention times according to $\log k' = \log(t_R - t_0)/t_0$; where t_R is the sample retention time, and t_0 is the mobile phase hold time as estimated by the retention time of MeOH used to dissolve each sample. For each standard and **2a–c** and **3a–c** compounds, a plot of $\log k'$ versus percentage of organic modifier (i.e., MeOH) was generated and extrapolated back to the 0% modifier in order to determine the capacity factor of each compound at 100% of buffer ($\log k'_w$).

Acknowledgments

This work was supported by grants from Secretaría de Ciencia y Técnica 162/2012, Ministerio de Ciencia y Tecnología, Gobierno de la Provincia de Córdoba 121/2008, Agencia Nacional de Promoción Científica y Tecnológica (ANPCyT) PICT 2006-1325 and 2010-0866, Consejo Nacional de Investigaciones Científicas y Técnicas (CONICET) PIP 0769 and Universidad de Buenos Aires UBACYT K066. Both M.M.N. and M.S.G. acknowledge receipt of a fellowship granted by Fondo Nacional de Promoción Científica y Tecnológica (FONCyT) and CONICET, respectively. M.A.R. and C.D.A.S. are members of the research career of CONICET. We thank Dr. Gloria Bonetto for her assistance in NMR data recording, Lic. MA Pino-Martinez and Lic. C. Miranda for the parasitemia determinations, and Dr. Paul Hobson, native speaker, for revision of the manuscript.

Appendix A. Supplementary material

Supplementary material associated with this article can be found, in the online version, at <http://dx.doi.org/10.1016/j.ejmech.2013.08.045>.

References

- [1] WHO, Chagas Disease (American Trypanosomiasis) Fact Sheet 340, August 2012. <http://www.who.int/mediacentre/factsheets/fs340/en/index.html>.
- [2] J. Gascon, C. Bern, M.J. Pinazo, Chagas disease in Spain, the United States and other non-endemic countries, *Acta Trop.* 115 (2010) 22–27.
- [3] C. Beyrer, J.C. Villar, V. Suwanvanichkij, S. Singh, S.D. Baral, E.J. Mills, Neglected diseases, civil conflicts, and the right to health, *Lancet* 370 (2007) 619–627.
- [4] J.A. Urbina, Specific chemotherapy of chagas disease: relevance, current limitations and new approaches, *Acta Trop.* 115 (2010) 55–68.
- [5] R. Viotti, C. Vigliano, B. Lococo, M.G. Alvarez, M. Petti, G. Bertocchi, A. Armenti, Side effects of benznidazole as treatment in chronic chagas disease: fears and realities, *Expert Rev. Anti Infect. Ther.* 7 (2009) 157–163.
- [6] J.D. Maya, B.K. Cassels, P. Iturriaga-Vásquez, J. Ferreira, M. Faúndez, N. Galanti, A. Ferreira, A. Morello, Mode of action of natural and synthetic drugs against *Trypanosoma cruzi* and their interaction with the mammalian host, *Comp. Biochem. Physiol. A* 146 (2007) 601–620.
- [7] F. Sánchez-Sancho, N.E. Campillo, J.A. Páez, Chagas disease: progress and new perspectives, *Curr. Med. Chem.* 17 (2010) 423–452.
- [8] W.E. Gutteridge, M.J. Davies, Enzymes of purine salvage in *Trypanosoma cruzi*, *FEBS Lett.* 127 (1981) 211–214.
- [9] W.N. Kelley, J.B. Wyngaarden, Effects of allopurinol and oxipurinol on purine synthesis in cultured human cells, *J. Clin. Invest.* 49 (1970) 602–609.
- [10] J.J. Marr, R.L. Berens, D.J. Nelson, Antitrypanosomal effect of allopurinol: conversion in vivo to aminopyrazolopyrimidine nucleotides by *Trypanosoma cruzi*, *Science* 201 (1978) 1018–1020.
- [11] R.L. Berens, J.J. Marr, F. Steele Da Cruz, D.J. Nelson, Effect of allopurinol on *Trypanosoma cruzi*: metabolism and biological activity in intracellular and bloodstream forms, *Antimicrob. Agents Chemother.* 22 (1982) 657–661.
- [12] R.H. Gallerano, J.J. Marr, R.R. Sosa, Therapeutic efficacy of allopurinol in patients with chronic chagas disease, *Am. J. Trop. Med. Hyg.* 43 (1990) 159–166.
- [13] P. Gobbi, M.S. Lo Presti, A.R. Fernandez, J.E. Enders, R. Fretes, S. Gea, P.A. Paglini-Oliva, H.W. Rivarola, Allopurinol is effective to modify the evolution of *Trypanosoma cruzi* infection in mice, *Parasitol. Res.* 101 (2007) 1459–1462.
- [14] A. Rassi, A. Ostermayer Luquetti, A. Rassi Jr., G.G. Rassi, S.G. Rassi, I. Garcia Da Silva, A.G. Rassi, Short report: specific treatment for *Trypanosoma cruzi*: lack of efficacy of allopurinol in the human chronic phase of chagas disease, *Am. J. Trop. Med. Hyg.* 76 (2007) 58–61.
- [15] D.E. Perez-Mazliah, M.G. Alvarez, G. Cooley, B.E. Lococo, G. Bertocchi, M. Petti, M.C. Albareda, A.H. Armenti, R.L. Tarleton, S.A. Laucella, R. Viotti, Sequential combined treatment with allopurinol and benznidazole in the chronic phase of *Trypanosoma cruzi* infection: a pilot study, *J. Antimicrob. Chemother.* 68 (2013) 424–437.
- [16] R.B. Bestetti, T.A.D. Theodoropoulos, A systematic review of studies on heart transplantation for patients with end-stage chagas' heart disease, *J. Card. Fail.* 15 (2009) 249–255.
- [17] N.L. Grosso, J. Bua, A.E. Perrone, M.N. Gonzalez, P.L. Bustos, M. Postan, L.E. Fichera, *Trypanosoma cruzi*: biological characterization of a isolate from an endemic area and its susceptibility to conventional drugs, *Exp. Parasitol.* 126 (2010) 239–244.
- [18] C.C. Cheng, R.K. Robins, Potential purine antagonist VII. Synthesis of 6-alkylpyrazolo-[3,4-d]pyrimidines, *J. Org. Chem.* 23 (1958) 191–200.
- [19] G. Biagi, A. Costantini, L. Costantino, I. Giorgi, O. Livi, P. Pecorari, M. Rinaldi, V. Scartoni, Synthesis and biological evaluation of new imidazole, pyrimidine, and purine derivatives and analogs as inhibitors of xanthine oxidase, *J. Med. Chem.* 39 (1996) 2529–2535.
- [20] H. Bundgaard, E. Falch, Allopurinol prodrugs I. Synthesis, stability and physicochemical properties of various N1-acyl allopurinol derivatives, *Int. J. Pharm.* 23 (1985) 223–237.
- [21] C.A. Lipinski, F. Lombardo, B.W. Dominy, P.J. Feeney, Experimental and computational approaches to estimate solubility and permeability in drug discovery and development settings, *Adv. Drug Deliv. Rev.* 46 (2001) 3–26.
- [22] A.J. Romanha, S.L. Castro, M.N. Soeiro, J. Lannes-Vieira, I. Ribeiro, A. Talvani, B. Bourdin, B. Blum, B. Olivieri, C. Zani, C. Spadafora, E. Chiari, E. Chetalain, G. Chaves, J.E. Calzada, J.M. Bustamante, L.H. Freitas-Junior, L.I. Romero, M.T. Bahia, M. Lotrowska, M. Soares, S.G. Andrade, T. Armstrong, W. Degraive, Z.A. Andrade, In vitro and in vivo experimental models for drug screening and development for chagas disease, *Mem. Inst. Oswaldo Cruz* 105 (2010) 233–238.
- [23] S.M. González-Cappa, A.T. Bijovsky, H. Freilij, L.A. Muller, A.M. Katzin, Isolation of a *Trypanosoma cruzi* strain of predominantly slender form in Argentina (Aislamiento de una cepa de *Trypanosoma cruzi* a predominio de formas delgadas en la Argentina), *Medicina* 41 (1981) 119–120.
- [24] G. Steele, T. Austin, Preformulation investigations using small amounts of compound as an aid to candidate drug selection and early development, in:

- M. Gibson (Ed.), Pharmaceutical Preformulation and Formulation, second ed., Informa Healthcare USA, Inc., New York, 2009, pp. 17–128.
- [25] M. Meloun, S. Bordovská, Benchmarking and validating algorithms that estimate $pK(a)$ values of drugs based on their molecular structures, *Anal. Bioanal. Chem.* 389 (2007) 1267–1281.
- [26] ICH, Stability testing of new drug substances and products Q1A (R2), in: Proceedings of the International Conference on Harmonisation, IFPMA, Geneva, 2003.
- [27] Guidance for Industry, Waiver of In Vivo Bioavailability and Bioequivalence Studies for Immediate Release Solid Oral Dosage Forms Based on a Biopharmaceutics Classification System, U.S. Department of Health and Human Services, Food and Drug Administration, Rockville, MD, USA, 2000.
- [28] Guidance for Industry, Bioanalytical, Method Validation, U.S. Department of Health and Human Services, Food and Drug Administration, Rockville, MD, USA, 2001.
- [29] A. Avdeef, Physicochemical profiling (solubility, permeability and charge state), *Curr. Top. Med. Chem.* 1 (2001) 277–351.
- [30] H. Tietgen, Physicochemical properties, in: H.G. Vogel, F.J. Hock, J. Maas, D. Mayer (Eds.), Drug Discovery and Evaluation. Safety and Pharmacokinetic Assay, Springer-Verlag, Berlin, Heidelberg, New York, 2006, pp. 399–408.
- [31] S.A. Benezra, T.R. Bennett, Allopurinol, in: K. Florey (Ed.), Analytical Profiles of Drug Substances V7, Acad. Press, New York, 1978, pp. 1–16.
- [32] A.T. Florence, D. Attwood, Physicochemical Principles of Pharmacy, fourth ed., Pharmaceutical Press, London, 2006, pp. 139–176.
- [33] A. Berthod, S. Carda-Broch, Determination of liquid–liquid partition coefficients by separation methods, *J. Chromatogr. A* 1037 (2004) 3–14.
- [34] Partition Coefficient (n-Octanol/Water), High Performance Liquid Chromatography (HPLC) Method, OECD Guideline for Testing of Chemicals, Test N° 117, 2004.
- [35] M.N. Nassar, T. Chen, M.J. Reff, S.N. Agharkar, Didanosine, in: K. Florey (Ed.), Analytical Profiles of Drug Substances and Excipients V22, Acad. Press, New York, 1993, pp. 185–227.
- [36] T. Braumann, Determination of hydrophobic parameters by reversed-phase liquid chromatography: theory, experimental techniques, and application in studies on quantitative structure–activity relationships, *J. Chromatogr.* 373 (1986) 191–225.
- [37] J. Selbo, P.C. Chiang, Absorption and physicochemical properties of the NCE, in: K. Tsaion, S.A. Kates (Eds.), ADMET for Medicinal Chemists: a Practical Guide, John Wiley & Sons, Inc., 2011, pp. pp125–144.
- [38] H. van de Waterbeemd, Physico-chemical approaches to drug absorption, in: H. van de Waterbeemd, H. Lennernäs, P. Artursson (Eds.), Drug Bioavailability: Estimation of Solubility, Permeability, Absorption and Bioavailability, Wiley-VCH, Weinheim, 2003, pp. 3–20.
- [39] P. Ertl, B. Rohde, P. Selzer, Fast calculation of molecular polar surface area as a sum of fragment-based contributions and its application to the prediction of drug transport properties, *J. Med. Chem.* 43 (2000) 3714–3717.
- [40] Test solutions, United States Pharmacopoeia 32/National Formulary 27, 2009.
- [41] M.C. Fernández, S.M. González Cappa, M.E. Solana, *Trypanosoma cruzi*: immunological predictors of benzimidazole efficacy during experimental infection, *Exp. Parasitol.* 124 (2010) 172–180.
- [42] J. Nakajima-Shimada, Y. Hirota, T. Aoki, Inhibition of *Trypanosoma cruzi* growth in mammalian cells by purine and pyrimidine analogs, *Antimicrob. Agents Chemother.* 40 (1996) 2455–2458.
- [43] L. Di, E.H. Kerns, Y. Hong, H. Chen, Development and application of high throughput plasma stability assay for drug discovery, *Int. J. Pharm.* 297 (2005) 110–119.